

Robust Distribution Alignment for Industrial Anomaly Detection under Distribution Shift

Jingyi Liao^{1,2}, Xun Xu¹, Yongyi Su³, Rong-Cheng Tu², Yifan Liu⁴, Dacheng Tao², Xulei Yang¹

¹Institute for Infocomm Research, A*STAR ²Nanyang Technological University

³South China University of Technology ⁴National University of Singapore

Abstract

Anomaly detection plays a crucial role in quality control for industrial applications. However, ensuring robustness under unseen domain shifts such as lighting variations or sensor drift remains a significant challenge. Existing methods attempt to address domain shifts by training generalizable models but often rely on prior knowledge of target distributions and can hardly generalise to backbones designed for other data modalities. To overcome these limitations, we build upon memory-bank-based anomaly detection methods, optimizing a robust Sinkhorn distance on limited target training data to enhance generalization to unseen target domains. We evaluate the effectiveness on both 2D and 3D anomaly detection benchmarks with simulated distribution shifts. Our proposed method demonstrates superior results compared with state-of-the-art anomaly detection and domain adaptation methods.

1. Introduction

Detecting anomalous patterns is essential for maintaining quality control in industrial applications. Current state-of-the-art methods for industrial anomaly detection typically require extensive defect-free training samples to model the distribution of normal patterns. These methods often employ reconstruction [12, 44] or memory banks [14, 19, 29, 38] to capture normal data distributions. While demonstrating impressive performance, they often overlook the robustness in real-world applications. In particular, domain shift, where training/source and testing/target data distributions¹ differ due to factors like changes in lighting or sensor drift, remain a significant challenge in industrial settings. Examples of synthesized distribution shift [16] are illustrated in Fig. 1 (upper). The performances of state-of-the-art methods are significantly compromised by the distribution shifts,

¹We respectively use training/source and testing/target interchangeably throughout the manuscript.

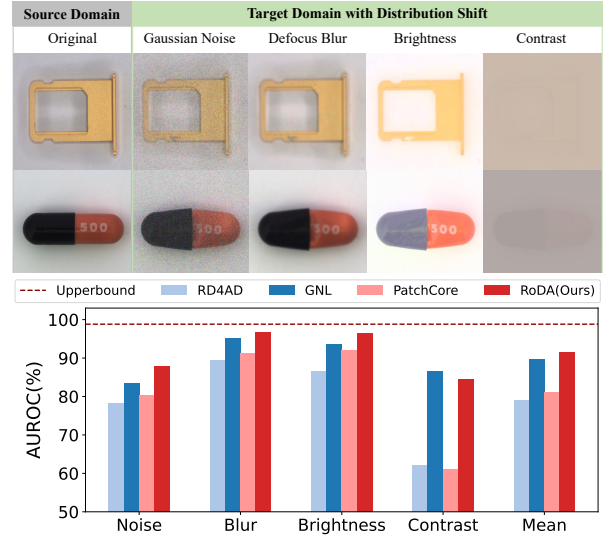


Figure 1. Upper: Examples of synthesized distribution shifts [16] on MVTec and ReaIAD. Lower: Results from top baselines and our method. The Upperbound is trained and tested on the original distribution. GNL [6] performs well on “Contrast” shift due to AutoContrast augmentation during training.

as evidenced by the gap between the “Upperbound” (results on clean testing data) and their performance on corrupted testing data.

Recent works [6, 21] tackle this issue by treating anomaly detection under distribution shift as an out-of-distribution (OOD) generalization problem. During training, they encourage consistency in the intermediate features of normal samples under different data augmentations, which is sometimes referred to as synthetic OOD by [21]. Training model with this objective ensures that the model’s representation is less sensitive to shifts in the data distribution at test time.

Despite recent advancements, domain generalization approaches face several key limitations. First, they rely on data augmentations or synthetic OOD samples that mimic target distribution shifts during training. This inherently as-

sumes prior knowledge of the target domain shift, which may not always hold. For example, GNL [6] suffers performance degradation when the actual distribution shift is not well represented by training augmentations. Second, these methods are built on reverse distillation [12], which requires *constructing a decoder to invert the encoder*. This design choice limits flexibility, making it non-trivial to extend to architectures such as 3D point cloud encoders. Finally, GNL [6] necessitates *access to a random normal training sample* at inference. However, privacy constraints and storage limitations often restrict access to training data, making this requirement impractical in real-world scenarios.

In this work, we first develop a memory-bank-based solution [29, 37] that overcomes limitations in modality, network architecture, and the reliance on normal training sample replay. Our approach extracts features from normal training samples and constructs a memory bank to capture their distribution. During inference, test sample features are compared against this memory bank, enabling anomaly detection without requiring a decoder or replaying normal samples. This design ensures broad generalization across different modalities and encoder architectures.

To further address the limitation of requiring prior knowledge of distribution shifts, we freeze the training stage with clean normal data and adapt the model using a small set of target adaptation data. In many scenarios, collecting some unlabeled target-domain data is feasible at low or no cost, enabling model adaptation. Domain adaptation methods [24, 25, 32, 33] leverage such data, with distribution alignment proving particularly effective. By modeling source and target distributions and minimizing their discrepancy, distribution alignment improves generalization with fewer hyperparameter sensitivities compared to self-training or self-supervised learning.

However, existing distribution alignment methods often overlook the presence of anomalies in target data which is common in anomaly detection tasks. Naively aligning distributions without accounting for anomalies can lead to misalignment, as anomalies may dominate the distribution discrepancy. To address this, we draw inspiration from robust distribution alignment techniques in generative modeling [1] and domain adaptation [8], formulating the adaptation process as an optimal transport problem. Given target training data, we compute a soft assignment between target samples and memory bank prototypes using optimal transport, e.g., the Sinkhorn distance [10]. To mitigate the risk of assigning anomalies to prototypes, we introduce two key techniques. First, we discretize/binarize the Sinkhorn assignment to suppress spurious alignments. We further conduct target domain augmentation to generate multiple views of target samples, increasing robustness to anomalies. These strategies enhance the robustness of Sinkhorn distance, ensuring more reliable adaptation.

These designs give rise to our method, **Robust Distribution Alignment (RoDA)** with an overview illustrated in Fig. 2. Finally, the adapted model is applied for inference on target test data, improving anomaly detection under distribution shifts.

Our contributions are summarized as follows.

- We identify the practical challenges of generalizing to OOD target data in industrial anomaly detection and propose a distribution alignment-based optimal transport approach to improve robustness.
- We enhance the optimal transport framework for anomaly detection by introducing assignment discretization and target domain data augmentation, mitigating the impact of anomalies.
- We conduct evaluations under synthetic distribution shifts across both 2D and 3D data modalities, demonstrating the effectiveness.

2. Related Works

Anomaly Detection: Anomaly Detection (AD) identifies samples that deviate significantly from the norm. Most AD approaches operate in an unsupervised setting, leveraging different techniques to model normal data [12, 12, 29, 30, 38, 40]. One-class classification methods, [26, 30], represent normal data using support samples. Reconstruction-based methods [40, 45] detect anomalies through higher reconstruction errors. Knowledge distillation approaches, such as RD4AD [12, 35], identify anomalies by comparing distilled and original features. Memory bank based methods [29, 42] measure deviations in feature space from normal training samples. Among these methods, memory bank based exhibits more versatility to different data modalities and network architectures due to the decoder-free architecture.

Domain Adaptation: Domain adaptation mitigates performance degradation caused by distribution shifts between training and testing data. Traditional methods, such as learning invariant representations [13] and clustering [34], rely on both source and target data, which is impractical when source data is restricted due to privacy concerns. This has driven interest in source-free [23–25, 32, 33, 39] and source-light [3, 33] adaptation, where models are updated without direct source access to enhance generalization. While effective for classification and segmentation, these methods struggle with anomaly detection. They typically model feature distributions using parametric assumptions (e.g., single Gaussian [25] or Gaussian mixtures [32, 33]) and align them via KL-Divergence or moment matching. However, fitting complex industrial data with simple distributions can lead to underfitting [25], and aligning without distinguishing anomalies can blur decision boundaries. Our method follows a source-light approach, leveraging a lightweight memory bank from source training data. We

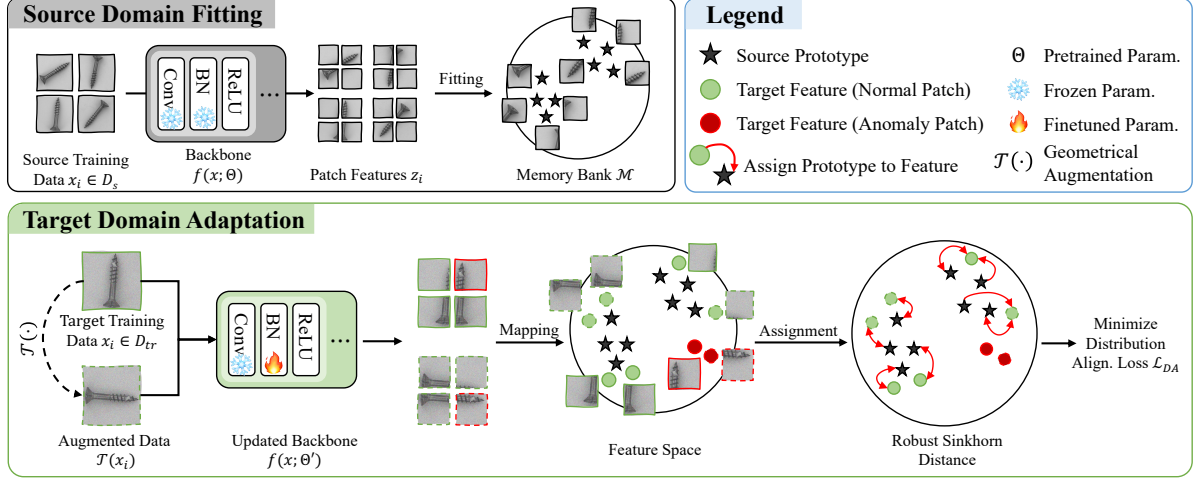


Figure 2. Illustration of pipeline of RoDA. The source domain fitting stage constructs a memory bank of normal training features, which serves as a reference for anomaly detection. In the domain adaptation stage, a limited amount of target domain data is augmented and aligned with the source memory bank through robust optimal transport.

optimize the optimal transport distance [10] between distributions, a widely studied technique in domain adaptation [8, 22], and extend it to handle outliers [2, 28]. Our approach improves efficiency and scalability by refining the Sinkhorn distance through discretization and target domain augmentation.

Anomaly Detection under Domain Shift: Anomaly detection under distribution shift has only recently gained attention [6, 21]. Existing attempts to address this challenge involved augmenting data during the training stage to enhance the model’s robustness [6, 21], demonstrating effectiveness in both industrial defect detection and natural OOD images. However, these approaches rely on the assumption that training can be modified and that prior knowledge of the distribution shift is available. In this work, we further relax these assumptions by updating the model only during test time upon observing target data, without modifying the training process. An alternative approach to handling anomaly detection under distribution shifts involves training from scratch using noisy target data [7, 20, 27]. These methods incrementally filter out potential anomalies and learn normal patterns from the remaining clean samples. Such methods may struggle to generalize when the noise level in the target distribution is high, limiting their effectiveness in handling severe distribution shifts, as demonstrated by the results in the Appendix.

3. Methodology

3.1. Problem Formulation

We first formally define the task of unsupervised anomaly detection under distribution shift. Without loss of generality, we denote the source domain training data as $\mathcal{D}_s = \{x_i, y_i\}_{i=1 \dots N_s}$ where all samples are defect-free. We further denote the target data as $\mathcal{D}_t = \{x_j, y_j\}_{j=1 \dots N_t}$

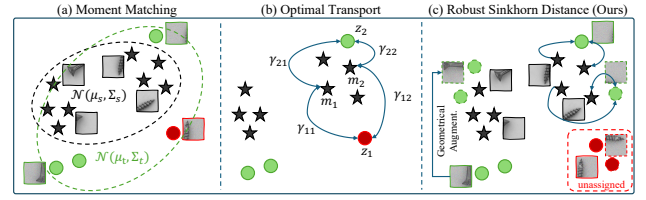


Figure 3. Illustration of distribution alignment via moment matching, optimal transport and finally our modified robust sinkhorn distance.

where the labels, y_j , are not visible. We split the target data into target training, \mathcal{D}_{tr} , and target testing, \mathcal{D}_{te} , i.e. $\mathcal{D}_t = \mathcal{D}_{tr} \cup \mathcal{D}_{te}$. The distributions from which samples are drawn write $\mathcal{D}_s \sim p_s$ and $\mathcal{D}_t \sim p_t$. For anomaly detection purpose, the label only takes a binary value, i.e. $y \in \{0, 1\}$ with 1 indicating anomalous.

Revisiting Memory-bank Based Anomaly Detection : Following the practice of memory bank based anomaly detection methods [29], a backbone network extracts features, $z_i = f(x_i; \Theta) \in \mathbb{R}^{N_p \times D}$, as N_p patches, from input sample x_i . A memory bank \mathcal{M} takes an abstraction of source domain training sample patches by sampling a core-set of size N_M as in Eq. 1.

$$\mathcal{M} = \arg \min_{\mathcal{M} \subset \mathcal{D}_s} \max_{z_j \in \mathcal{D}_s} \min_{m_i \in \mathcal{M}} \|m_i - z_j\|, \quad (1)$$

$$\text{s.t. } |\mathcal{M}| \leq N_M.$$

At inference stage, testing sample features are compared against the memory bank to determine anomaly as follows.

$$s_i = \max_{p \in 1 \dots N_p} \min_{m_k \in \mathcal{M}} \|z_{ip} - m_k\|. \quad (2)$$

The above procedure achieves competitive results for industrial defect identification.

3.2. Distribution Alignment for Domain Adaptation

Under the vanilla memory bank based anomaly detection, we witness a significant performance drop when testing data experiences a distribution shift, i.e. $p_s \neq p_t$. The mismatch results in an overall increase of anomaly scores s_i . The increment of score is often non-deterministic and inhomogeneous among patches, i.e., anomaly scores for normal and abnormal patches do not simply increase linearly, resulting in unreliable predictions using original PatchCore [29], which assumes *i.i.d.* test set.

Distribution Alignment via Moment Matching: Without knowing the target domain distribution shift in advance, recent works proposed distribution alignment to mitigate the distribution shift [25, 32, 33]. Specifically, a parametric distribution, e.g. multi-variate Gaussian distribution [25] or mixture of Gaussian distributions [32, 33], is fitted on both source and target domain, denoted as $p_s(z)$ and $p_t(z)$. A loss function that measures the discrepancy between $p_s(z)$ and $p_t(z)$ is employed. For example, [25] introduced minimizing the L2 distance between mean and covariance between the two Gaussian distributions (moment matching) for alignment as in Eq. 3.

$$\min_{\Theta} \mathcal{L}_{DA}, \quad \text{s.t.} \quad \mathcal{L}_{DA} = \|\mu_s - \mu_t\|_2^2 + \|\Sigma_s - \Sigma_t\|_F^2. \quad (3)$$

Despite the success for classification tasks, we argue that such a vanilla distribution alignment approach is suboptimal for memory bank based anomaly detection task due to the following reasons. As shown in Fig. 3 (a), without knowing the prior information of the feature distribution, fitting arbitrary sample features with a single multi-variate Gaussian distribution is prone to underfitting. A mixture of Gaussian distributions may better fit the complex distribution, however, this requires complicated approximations for KL-Divergence [17]. Moreover, target distribution is fitted on target domain contaminated with anomalies. Aligning the target distribution with source distribution will undermine the discrimination between normal and abnormal samples.

Distribution Alignment via Optimal Transport: Inspired by the success of distribution based via optimal transport for unsupervised domain adaptation [9, 11], we propose to use optimal transport (OT) distance for robust distribution alignment between \mathcal{M} and \mathcal{D}_{tr} . Specifically, a cost matrix $C \in \mathbb{R}^{N_{tp} \times N_M}$ is built between target training patches and source memory bank with $C_{ij} = \|z_i - m_j\|$ and $N_{tp} = N_t \cdot N_p$. Assuming uniform weight applied to each sample, the optimal transport is formulated as,

$$\begin{aligned} & \min_{\gamma \geq 0} \sum_i \sum_j \gamma_{ij} C_{ij}, \\ \text{s.t.} \quad & \sum_i \gamma_{ij} = \frac{1}{N_M}, \quad \sum_j \gamma_{ij} = \frac{1}{N_{tp}}. \end{aligned} \quad (4)$$

Solving the above problem, through linear programming, is expensive and an efficient algorithm, Sinkhorn distance [10], exists that can substantially reduce the computation cost. Specifically, an entropy regularization term is added to improve the smoothness and robustness of solution, as in Eq. 5. An iterative algorithm is employed to solve the problem with details explained in the supplementary.

$$\begin{aligned} & \min_{\gamma \geq 0} \sum_i \sum_j \gamma_{ij} C_{ij} + \epsilon \sum_i \sum_j \gamma_{ij} \log \gamma_{ij}, \\ \text{s.t.} \quad & \sum_i \gamma_{ij} = \frac{1}{N_M}, \quad \sum_j \gamma_{ij} = \frac{1}{N_{tp}}. \end{aligned} \quad (5)$$

A Self-Training Perspective: We further elaborate the distribution alignment from a self-training (ST) perspective. ST has been demonstrated to be effective for domain adaptation [33]. The regular routine makes predictions on target domain samples and use most confident ones, a.k.a. pseudo labels, to train network, e.g. optimize cross-entropy loss for classification task. In the realm of anomaly detection, self-training could translate into encouraging target domain patch to be close to the closest patch in the memory bank. Distribution alignment via optimal transport can be seen as discovering a global optimal assignment between target patches and memory bank, as in Fig. 3 (b). The assignment can be seen as the pseudo label and minimizing the earth moving distance is equivalent to using the pseudo label for self-training.

3.3. Robust Sinkhorn Distance

Solving the optimal transport problem in Eq. 5 yields the assignment γ^* for each target sample to source samples. The Sinkhorn distance, $\mathcal{L}_{DA} = \sum_i \sum_j \gamma_{ij}^* C_{ij}$, could be adopted as the objective to optimize for distribution alignment. However, we notice an unresolved issue by directly optimizing the above objective. First, an anomalous patch, indexed by j^* , in the target domain are always assigned to source patches in the memory bank due to the constraint $\gamma_{ij^*} \geq 0$, $\sum_i \gamma_{ij^*} = \frac{1}{N_M}$. Minimizing the distance between anomalous patches and memory bank patches will inevitably diminish the discriminability. To improve the robust of optimal transport for distribution alignment, we convert the continuous optimal transport assignment into discrete assignment. Fortunately, the discretization may eliminate weak assignments that often appear on anomalous patches in the target domain. Specifically, we follow the rules below to discretize the assignment, resulting in a more robust distribution alignment loss in Eq. 6.

$$\min_{\Theta} \mathcal{L}_{DA}, \quad \text{s.t.} \quad \mathcal{L}_{DA} = \sum_i^{N_{tp}} \sum_j^{N_M} \pi_{ij}^* C_{ij}, \quad (6)$$

$$\pi_{ij}^* = \begin{cases} 1 & \text{if } j = \arg \max_j \gamma_{ij}^*, \text{ or } i = \arg \max_i \gamma_{ij}^*, \\ 0 & \text{otherwise.} \end{cases}$$

Target Domain Data Augmentation: We apply a batch-wise update strategy to facilitate gradient based update of backbone weights. Within each minibatch we further apply data augmentation $\mathcal{T}(x)$ on the target training data to improve the effectiveness distribution alignment, $\tilde{\mathcal{D}}_t = \{\mathcal{T}(x_j)\}_{j=1 \dots N_t}$. The augmentation simulates the normal data variation, e.g. rotation in multiple of 90° , etc. Importantly, the augmentation is agnostic to the corruption (distribution shift) on the target domain and is only applied at adaptation stage, in contrast to the training stage augmentation adopted in [6, 21]. We attribute the effectiveness of test-time target domain augmentation to the following reasons. First, the augmentation will create a more diverse and smoother distribution. This can help mitigate the impact of outliers by “diluting” their influence, making the alignment focus on general features rather than outlier-specific characteristics. Moreover, data augmentation can help by incorporating additional noise into the training process in a controlled way, making the model more resilient to noise and outliers in the real world. Fig. 3 (c) has shown the main differences between our robust sinkhorn distance and the previous methods. The positive effect is demonstrated by the reduced discretised assignment, as in Fig. 5 (a).

3.4. Overall Algorithm

Following the practice of common test-time training strategies, we update the batchnorm affine parameters, Θ_{bn} , with distribution alignment loss. We present the overall algorithm of the proposed method in Algo. 1.

4. Experiments

4.1. Experiment Settings

Dataset: We evaluate our method on two widely-used 2D industrial anomaly detection datasets, **MVTec** [4] and **RealIAD** [36], as well as on a 3D dataset, **MVTec 3D** [5]. **MVTec** is the most commonly used benchmark for 2D industrial anomaly detection, comprising 15 object categories, with 60-300 normal samples for training and 30-400 normal and anomalous samples for testing. **RealIAD** is a newly introduced industrial dataset with 30 object categories, each captured from five different viewpoints. We follow the single-view experiment setup, utilizing only the top-view images. Due to the high resolution of the original images (over 3,000×5,000 pixels), which imposes significant computational demands, we use a downsampled ver-

Algorithm 1 Domain Adaptation for Anomaly Detection

- 1: **Input:** Pretrained memory bank \mathcal{M} , target training data \mathcal{D}_{tr} , target testing data \mathcal{D}_{te} , initial encoder network Θ
 - 2: **Output:** Anomaly scores $\{s_i\}$
Domain Adaptation on target training data
 - 3: **for** $\mathcal{B}_t \subset \mathcal{D}_{tr}$ **do** # Collect one minibatch \mathcal{B}_t
 Augment target minibatch $\tilde{\mathcal{B}}_t = \mathcal{T}(\mathcal{B}_t)$
 Compute cost matrix $C \in \mathbb{R}^{|\mathcal{D}_s| \times |\tilde{\mathcal{B}}_t|}$
 Solve optimal transport plan γ^* by Eq. 5
 Discretize assignment π^* by Eq. 6
 Update model $\Theta_{bn} = \Theta_{bn} - \alpha \frac{\nabla \mathcal{L}_{DA}}{\Theta_{bn}}$
 - 4: **end for**
Evaluate on target testing data
 - 5: **for** $x_i \in \mathcal{D}_{te}$ **do**
 Encode feature with updated model $z_i = f(x_i; \Theta^*)$
 Per sample anomaly score $s_i = \max_{p \in 1 \dots N_p} \min_{m_k \in \mathcal{M}} \|z_{ip} - m_k\|_2$
 - 6: **end for**
 - 7: **return** s_i
-

sion with a resolution of 1,024×1,024. **MVTec 3D** consists of 3D scans that include both geometric surface data and RGB information. The dataset comprises 10 object categories, with over 200 normal images for training and more than 100 images for testing per category.

Evaluation Protocol: We simulate commonly seen distribution shift in the testing set to evaluate the generalization robustness. For the 2D datasets, **MVTec** and **RealIAD**, we follow the corruption generation process described in [16], applying four common corruptions, including Gaussian Noise, Defocus Blur, Contrast, and Brightness, with a severity level of 5 to synthesize distribution-shifted data. In the 3D dataset, **MVTec 3D**, we simulate natural distribution shifts by randomly adding Gaussian noise $n \sim \mathcal{N}(0, [1e - 6]^2)$ to the images.

The distribution shifted test set is then split into two parts: 20% for model adaptation and 80% for final evaluation. To ensure a fair comparison, all baseline methods are evaluated on the same 80% test set. We assess the performance using the area under the ROC curve (AUROC), treating anomalies as the positive class for both anomaly detection and segmentation tasks, following the standard protocol [4]. The remaining experimental settings are provided in the Appendix.

Competing Methods: We compare against several baseline methods, covering several state-of-art industrial AD methods, and three domain adaptation AD methods. These 2D industrial AD methods including reconstruction-based approaches (**ViTAD** [43]), embedding-based meth-

ods (**CFLOW-AD** [15]), and knowledge distillation methods (**KDAD** [31] and **RD4AD** [12]). We also evaluated on a unified model (**UniAD** [41]), and the effective memory-bank-based method (**PatchCore** [29]). We further incorporate domain adaptation methods for anomaly detection task. In specific, we evaluated two distribution alignment based approaches, **TTT++** [25] and **TTAC** [32], on top of PatchCore. Additionally, the state-of-the-art domain adaptation method for anomaly detection, **GNL** [6], are benchmarked. We allow GNL to be trained with default data augmentation. For 3D anomaly detection, we also benchmark several hand-crafted features implemented by [5], FPFH [18] and M3DM [37]. Finally, we evaluate our proposed method, **RoDA**, on all datasets.

4.2. Distribution Shifted Anomaly Detection

We first present the anomaly detection results, averaged across all object classes, on both the MVTEC and ReallAD datasets in Tab. 1. More detailed results for per-class AUROC are deferred to the Appendix. From the results, we make the following key observations. **i)** State-of-the-art anomaly detection methods struggle significantly under distribution shifts, as evidenced by the performance gap when tested on clean versus corrupted target data. For instance, PatchCore shows a performance drop of 18.58% when exposed to Gaussian noise on the MVTEC dataset. This highlights the vulnerability of these methods to out-of-distribution (OOD) scenarios. **ii)** Domain adaptation methods (e.g., TTT++ and TTAC), despite showing strong performance on classification tasks, fall short on anomaly detection. TTAC generally underperforms compared to PatchCore, and while TTT++ improves on MVTEC, it struggles on the more challenging RealAd dataset. This can be attributed to their reliance on modeling complex distributions with a single Gaussian, which is underfitting. **iii)** In contrast, RoDA, which leverages distribution alignment via optimal transport, demonstrates superior performance in 3 out of 4 types of corruptions, with the sole exception being the “Contrast” corruption. Notably, under the “Defocus Blur” and “Brightness” corruptions on the MVTEC dataset, RoDA’s performance is only 2% behind the results on source domain. These findings underscore the importance of a well-calibrated distribution strategy for robust anomaly detection. **iv)** Lastly, we observe that GNL significantly outperforms all competing methods under the “Contrast” corruption scenario. Upon further investigation, we discovered that GNL employs an “AutoContrast” augmentation during training on source domain, which inadvertently provides prior knowledge of the target data distribution. This advantage highlights the importance of evaluating methods under consistent and unbiased conditions.

In addition to the experiments on 2D data, we also evaluated our method on 3D data by introducing Gaussian

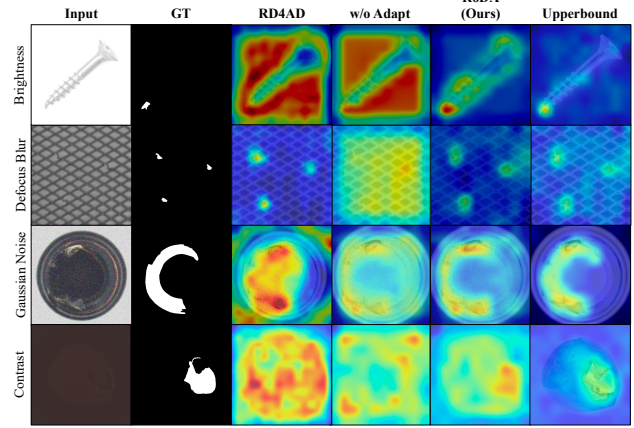


Figure 4. Qualitative results for anomaly segmentation. We present results for PatchCore without adaptation (w/o Adapt), RD4AD, RoDA (Ours) and predictions on original distribution testing sample as Upperbound. RoDA consistently improves anomaly localization compared to the baseline (w/o Adapt), even approaching the Upperbound in some cases.

noise as a form of corruption. The results are presented in Tab. 2. Compared to standard 2D corruptions, adding Gaussian noise to 3D data introduces a greater challenge. The geometric structures in 3D data are particularly sensitive to noise, as it disrupts fine details and depth information, both of which are crucial for effective 3D anomaly detection. Despite these challenges, our method demonstrates resilience, achieving a notable performance improvement of 14.21% on PointMAE. Compared with other adaptation methods, our approach achieves a 2.33% improvement over the second-best TTT++ adaptation. This suggests that our approach is capable of effectively managing the complexities introduced by noise in 3D data, maintaining robust anomaly detection capabilities.

4.3. Distribution Shifted Anomaly Segmentation

We also evaluate the anomaly segmentation performance on the MVTEC and ReallAD dataset, with the results summarized in Tab. 3. Detailed results for each class are deferred to the Appendix. For a fair comparison, we include only those methods that provide segmentation solutions in their original papers. As shown in the table, our method consistently achieves superior AUROC across all types of corruption in the segmentation task. Notably, it surpasses all baseline methods across different corruptions on both dataset. While TTT++ also performs well under Defocus Blur on MVTEC dataset, our method maintains an advantage. Moreover, under Contrast on MVTEC dataset, our approach outperforms TTT++ by significant margins of 9.16%. On the ReallAD dataset, our method further shows a significant lead in the all corruption types.

Qualitative Results: We provide a qualitative comparison of anomaly segmentation results, as shown in Fig. 4.

Table 1. Results of anomaly detection on MVTec and ReallAD datasets. We report the mAUROC(%) averaged across all classes. “Clean” refers to the results on testing samples without distribution shift.

		MVTec						ReallAD					
		Clean	Gauss. Noise	Defoc. Blur	Bright.	Contrast	Mean	Clean	Gauss. Noise	Defoc. Blur	Bright.	Contrast	Mean
w/o adapt.	ViTAD [43]	98.30	64.91	80.15	65.67	54.07	66.20	82.70	52.50	73.46	60.90	57.21	61.02
	KDAD [31]	87.74	72.18	79.33	70.98	47.65	67.54	80.23	41.43	31.15	38.36	46.80	39.44
	RD4AD [12]	98.50	78.09	89.45	86.55	62.02	79.03	86.17	56.57	79.55	63.65	57.56	64.33
	UnIAD [41]	92.50	82.00	91.00	85.33	60.13	79.61	83.10	64.21	78.81	69.41	54.07	66.63
	CFLOW-AD [15]	91.55	60.69	60.23	55.88	51.45	57.06	77.00	56.45	62.59	56.38	53.24	57.17
	PatchCore [29]	98.81	80.23	91.22	91.91	60.89	81.06	90.35	60.27	76.75	62.60	49.65	62.32
w/ adapt.	TTAC [32]	98.81	58.99	81.49	57.43	56.49	63.60	90.35	52.11	50.73	44.53	50.52	49.47
	TTT++ [25]	98.81	84.06	94.61	93.32	71.52	85.88	90.35	62.96	72.09	62.68	57.21	63.74
	GNL [6]	97.99	83.26	95.18	93.55	86.50	89.62	83.44	68.80	73.78	68.90	62.26	68.44
	RoDA (Ours)	98.81	87.92	96.56	96.44	84.45	91.34	90.35	72.48	80.11	71.17	60.22	71.00

Table 2. Results of anomaly detection on MVTec-3D with per class AUROC(%)

		Bagel	CableGland	Carrot	Cookie	Dowel	Foam	Peach	Potato	Rope	Tire	Mean
w/o adapt.	Depth GAN [5]	47.5	24.0	49.1	45.9	37.4	36.8	32.4	37.0	35.1	36.5	38.17
	Depth AE [5]	33.4	38.6	43.3	47.9	40.7	32.3	42.9	41.6	41.2	38.3	40.02
	Depth VM [5]	36.7	32.2	37.4	44.6	40.4	29.2	38.7	29.5	45.3	39.7	37.37
	Depth PatchCore [29]	75.8	53.8	64.3	75.5	44.6	48.4	40.8	50.7	56.5	56.6	56.70
	Raw (in BTF) [5]	58.4	49.8	44.8	45.7	50.2	33.2	24.7	31.1	44.6	50.4	43.29
	HoG (in BTF) [5]	61.2	57.2	33.0	56.9	51.1	41.8	38.4	69.2	50.0	60.6	51.94
	SIFT (in BTF) [5]	46.1	42.3	44.1	46.6	38.5	41.9	33.4	55.7	62.4	56.4	46.74
	FPFH [18]	49.4	48.0	54.8	37.0	38.8	38.7	36.5	50.7	51.9	49.8	45.56
	M3DM [37]	74.1	51.6	73.2	83.2	59.9	58.6	30.0	76.3	86.8	70.8	66.45
w/ adapt.	TTAC [32]	68.1	65.9	90.8	87.0	74.0	52.8	60.5	81.3	84.9	41.6	70.69
	TTT++ [25]	91.2	71.4	93.4	88.9	75.1	65.6	66.4	86.7	82.2	62.4	78.33
	RoDA (Ours)	92.2	69.2	92.6	94.5	82.1	70.6	73.4	83.2	82.6	66.2	80.66

We compare our method with PatchCore without adaptation and the second-best overall adaptation-free baseline, RD4AD. The source predictions serve as reference upper-bound. RD4AD performs well under simpler corruptions like Defocus Blur, achieving relatively accurate anomaly localization. However, under more challenging corruptions such as Brightness and Contrast, it tends to misidentify the entire background or object as the anomaly area. In contrast, our method shows a significant improvement compared to the no-adaptation model, which lacks segmentation capability, and demonstrate a strong and consistent performance which is closely approaching the upper bound results on clean samples.

4.4. Ablation Study

Component Effectiveness: We analyze the effectiveness of proposed methods by investigating distribution alignment method, assignment method and target data augmentation. The ablation study carried out on MVTec dataset is presented in Tab. 4. We make the following observations from the results. **i)** KL-Div [33] and Moment Matching [25]-based alignment exhibit the poorest performance across all corruption types. For example, under Gaussian Noise, KL-div achieves only 58.99% in image-level AUROC. This indicates that these alignment methods are not well-suited for handling complex distribution shifts in anomaly detection tasks. In contrast, optimal Transport-based alignment

consistently outperforms KL-Div and Moment Matching across all corruptions. **ii)** We further compared with another way of discrete optimal transport solution, i.e. using Hungarian Method to find linear assignment between memory bank and target samples. Introducing Hungarian Method assignment for Optimal Transport yields better results compared to KL-Div. and Moment Matching distribution alignment, as seen in the case of Brightness and Contrast. **iii)** We compare with optimizing the earth moving distance as training objective, denoted as “Continuous” under Assignment. The earth moving distance can be derived from the continuous solution, γ , to optimal transport solution as $\sum_i \sum_j \gamma_{ij}^* C_{ij}$. We observe that using the robust sinkhorn distance (discretized) is consistently better than the continuous version. **iv)** When directly copying the target data for augmentation, the performance improves further, particularly in pixel-wise AUROC. Applying data augmentation instead of direct copying results in the best performance overall.

In summary, the best-performing configuration combines Optimal Transport alignment with discrete assignment and data augmentation, achieving top scores in both instance-level and pixel-wise AUROC across all corruption types. Notably, the Contrast corruption is still posing great challenge to the method which is explained by the low visibility of defects. In contrast, the KL-Div and Moment Matching methods generally underperform, indicating that

Table 3. Anomaly segmentation results on MVTec and ReaIIAD datasets. We report the pixel-level P-mAUROC(%) across all classes.

		MVTec						ReaIIAD					
		Clean	Gauss. Noise	Defoc. Blur	Brightness	Contrast	Mean	Clean	Gauss. Noise	Defoc. Blur	Brightness	Contrast	Mean
w/o adapt.	CFLOW-AD [15]	95.65	70.40	78.87	75.55	52.90	69.43	88.60	71.30	91.08	85.05	72.21	79.91
	UnIAD [41]	95.70	71.04	87.37	90.74	72.62	80.44	86.00	88.12	96.15	90.20	80.66	88.78
	RD4AD [12]	97.80	86.99	93.89	91.64	77.69	87.55	89.22	62.51	93.63	78.31	79.98	78.61
	PatchCore [29]	98.34	88.89	94.30	92.77	71.09	86.76	98.10	76.39	96.61	83.03	74.08	82.53
w/ adapt.	TTAC [32]	98.34	57.14	82.57	40.96	54.84	58.88	98.10	52.90	45.91	62.40	50.18	52.85
	TTT++ [25]	98.34	91.09	96.69	94.61	79.79	90.55	98.10	75.35	90.22	78.67	68.16	78.10
	RoDA (Ours)	98.34	92.26	97.05	96.47	88.95	93.68	98.10	93.14	97.81	91.85	84.19	91.75

Table 4. Ablation study on MVTec dataset. We report anomaly detection and segmentation AUROC averaged over all classes (mAUCROC & P-mAUROC).

Distribution Alignment	Assignment	Target Data Aug.	Gaussian Noise		Defocus Blur		Brightness		Contrast	
			mAUCROC	P-mAUROC	mAUCROC	P-mAUROC	mAUCROC	P-mAUROC	mAUCROC	P-mAUROC
-	-	-	80.23	88.89	91.22	94.30	91.91	92.77	60.89	71.09
KL-Diver.	-	-	58.99	57.14	81.49	82.57	57.43	40.96	56.49	54.84
Moment Matching	-	-	84.06	91.09	94.61	96.69	93.32	94.61	71.52	79.79
Optimal Transport	Hun. Method	-	82.95	88.77	93.13	95.60	93.75	94.23	72.80	80.61
Optimal Transport	Continuous	-	82.51	89.10	92.55	95.39	94.16	95.61	76.01	83.21
Optimal Transport	Discrete	-	84.40	91.50	94.62	96.01	94.43	95.71	76.63	82.95
Optimal Transport	Discrete	Direct Copy	84.47	91.55	94.64	96.04	94.41	95.65	76.65	83.01
Optimal Transport	Discrete	Data Augment.	87.92	92.26	96.56	97.05	96.44	96.47	84.45	88.95

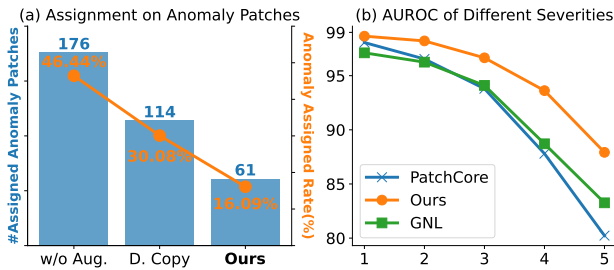


Figure 5. (a) Comparison of anomaly sample assignments across different strategies. (b) Evaluation on different severity levels of Gaussian Noise Corruption.

more sophisticated distribution alignment techniques, like Optimal Transport, are critical for handling complex distribution shifts in anomaly detection tasks.

Target Data Augmentation: We further demonstrate the effectiveness of the proposed augmentation method by analyzing the anomaly sample assignments in the optimal transport solutions within the same batch. As illustrated in Fig. 5 (a), out of total 376 anomaly patches, the number of assigned patches significantly decreased from 176 (46.44%) to 61 (16.09%) when applying our data augmentation strategy. This reduction highlights the method’s ability to limit erroneous anomaly assignments, thereby enhancing the quality of the optimal transport solution. Additionally, we evaluate the impact of simply duplicating the target data for augmentation, which led to a slight reduction in anomaly assignments to 114 (30.08%). We attribute this minor improvement to the larger selection pool, though this approach fails to smooth the distribution effectively.

Robustness on Different Severity: We evaluated the robustness of our method across different corruption severity levels. Fig. 5 (b) compares the image level AUROC performance of PatchCore, GNL, and RoDA under Gaus-

sian Noise corruption of increasing severity (levels 1 to 5). While all methods exhibit a performance decline as noise severity grows, our method consistently outperforms both PatchCore and GNL at every severity level. Notably, the performance gap becomes more pronounced under higher noise levels, indicating that our approach is more robust to extreme distribution shifts.

Amount of Target Training Data: We examine the impact of varying the target training data size. As shown in Tab. 5, our default setting uses 20% of the total target domain data for adaptation, with the remaining 80% reserved for testing. The “80%” setting reverses this split, while the “100%” setting adapts on the entire target domain data, establishing an upper bound on performance. Remarkably, using just 20% of the data achieves over 98% of the upper bound performance, highlighting our method’s robustness even with limited target data.

Table 5. Anomaly detection results on MVTec dataset with different amount of target training data. mAUCROC (%) averaged across all classes.

$ \mathcal{D}_{tr} / \mathcal{D}_t $	G. Noise	D. Blur	Bright.	Contrast	Mean
20%	87.92	96.56	96.44	84.45	91.34
80%	89.40	97.82	97.70	85.01	92.48
100%	90.33	97.81	97.88	85.45	92.87

5. Conclusion

In this work, we addressed a realistic challenge of deploying anomaly detection model to target domain with distribution shift. Existing works require modifying training objective and require access source domain data during inference to improve robustness. We relaxed these assumptions by proposing a robust distribution alignment method to mitigate the distribution shift. In particular,

a robust Sinkhorn distance is adapted from an existing optimal transport problem to improve the resilience to anomalous patches in the target domain data. We also introduce target data augmentation to reduce the assignment of anomalous patches. We demonstrated the effectiveness on three industrial anomaly detection datasets. The findings suggest future research should pay more attention to the robustness of anomaly detection under realistic challenges.

References

- [1] Jonas Adler and Sebastian Lunz. Banach wasserstein gan. *Advances in Neural Information Processing Systems*, 2018. 2
- [2] Yogesh Balaji, Rama Chellappa, and Soheil Feizi. Robust optimal transport with applications in generative modeling and domain adaptation. *Advances in Neural Information Processing Systems*, 2020. 3
- [3] Mathilde Bateson, Hoel Kervadec, Jose Dolz, Hervé Lombaert, and Ismail Ben Ayed. Source-relaxed domain adaptation for image segmentation. In *Medical Image Computing and Computer Assisted Intervention*, 2020. 2
- [4] Paul Bergmann, Michael Fauser, David Sattlegger, and Carsten Steger. Mvtec ad—a comprehensive real-world dataset for unsupervised anomaly detection. In *IEEE/CVF Conference on Computer Vision and Pattern Recognition*, 2019. 5
- [5] Paul Bergmann, Xin Jin, David Sattlegger, and Carsten Steger. The mvtec 3d-ad dataset for unsupervised 3d anomaly detection and localization. *VISAPP*, 2021. 5, 6, 7
- [6] Tri Cao, Jiawen Zhu, and Guansong Pang. Anomaly detection under distribution shift. In *IEEE/CVF International Conference on Computer Vision*, 2023. 1, 2, 3, 5, 6, 7
- [7] Yuanhong Chen, Yu Tian, Guansong Pang, and Gustavo Carneiro. Deep one-class classification via interpolated gaussian descriptor. In *AAAI Conference on Artificial Intelligence*, 2022. 3
- [8] Nicolas Courty, Rémi Flamary, Devis Tuia, and Alain Rakotomamonjy. Optimal transport for domain adaptation. 2016. 2, 3
- [9] Nicolas Courty, Rémi Flamary, Amaury Habrard, and Alain Rakotomamonjy. Joint distribution optimal transportation for domain adaptation. *Advances in Neural Information Processing Systems*, 2017. 4
- [10] Marco Cuturi. Sinkhorn distances: Lightspeed computation of optimal transport. *Advances in Neural Information Processing Systems*, 2013. 2, 3, 4
- [11] Bharath Bhushan Damodaran, Benjamin Kellenberger, Rémi Flamary, Devis Tuia, and Nicolas Courty. Deepjdot: Deep joint distribution optimal transport for unsupervised domain adaptation. In *European Conference on Computer Vision*, 2018. 4
- [12] Hanqiu Deng and Xingyu Li. Anomaly detection via reverse distillation from one-class embedding. In *IEEE/CVF Conference on Computer Vision and Pattern Recognition*, 2022. 1, 2, 6, 7, 8
- [13] Yaroslav Ganin and Victor Lempitsky. Unsupervised domain adaptation by backpropagation. In *International Conference on Machine Learning*, 2015. 2
- [14] Zhihao Gu, Liang Liu, Xu Chen, Ran Yi, Jiangning Zhang, Yabiao Wang, Chengjie Wang, Annan Shu, Guannan Jiang, and Lizhuang Ma. Remembering normality: Memory-guided knowledge distillation for unsupervised anomaly detection. In *IEEE/CVF International Conference on Computer Vision*, 2023. 1
- [15] Denis Gudovskiy, Shun Ishizaka, and Kazuki Kozuka. Cflow-ad: Real-time unsupervised anomaly detection with localization via conditional normalizing flows. In *IEEE/CVF Winter Conference on Applications of Computer Vision*, 2022. 6, 7, 8
- [16] Dan Hendrycks and Thomas Dietterich. Benchmarking neural network robustness to common corruptions and perturbations. In *International Conference on Learning Representations*, 2019. 1, 5
- [17] John R Hershey and Peder A Olsen. Approximating the kullback leibler divergence between gaussian mixture models. 2007. 4
- [18] Eliahu Horwitz and Yedid Hoshen. An empirical investigation of 3d anomaly detection and segmentation. *arXiv preprint*, 2022. 6, 7
- [19] Jianlong Hu, Xu Chen, Zhenye Gan, Jinlong Peng, Shengchuan Zhang, Jiangning Zhang, Yabiao Wang, Chengjie Wang, Liujuan Cao, and Rongrong Ji. Dmad: Dual memory bank for real-world anomaly detection. *arXiv preprint*, 2024. 1
- [20] Xi Jiang, Jianlin Liu, Jinbao Wang, Qiang Nie, Kai Wu, Yong Liu, Chengjie Wang, and Feng Zheng. Softpatch: Unsupervised anomaly detection with noisy data. *Advances in Neural Information Processing Systems*, 2022. 3
- [21] Hossein Kashiani, Niloufar Alipour Talemi, and Fatemeh Afghah. Roads: Robust prompt-driven multi-class anomaly detection under domain shift. In *IEEE/CVF Winter Conference on Applications of Computer Vision*, 2025. 1, 3, 5
- [22] Chen-Yu Lee, Tanmay Batra, Mohammad Haris Baig, and Daniel Ulbricht. Sliced wasserstein discrepancy for unsupervised domain adaptation. In *IEEE/CVF Conference on Computer Vision and Pattern Recognition*, 2019. 3
- [23] Jian Liang, Dapeng Hu, and Jiashi Feng. Do we really need to access the source data? source hypothesis transfer for unsupervised domain adaptation. In *International Conference on Machine Learning*, 2020. 2
- [24] Jian Liang, Dapeng Hu, Yunbo Wang, Ran He, and Jiashi Feng. Source data-absent unsupervised domain adaptation through hypothesis transfer and labeling transfer. *IEEE Transactions on Pattern analysis and Machine Intelligence*, 2021. 2
- [25] Yuejiang Liu, Parth Kothari, Bastien Van Delft, Baptiste Bellot-Gurlet, Taylor Mordan, and Alexandre Alahi. Ttt++: When does self-supervised test-time training fail or thrive? In *Advances in Neural Information Processing Systems*, 2021. 2, 4, 6, 7, 8
- [26] Zhikang Liu, Yiming Zhou, Yuansheng Xu, and Zilei Wang. SimpNet: A simple network for image anomaly detection

- and localization. In *IEEE/CVF Conference on Computer Vision and Pattern Recognition*, 2023. 2
- [27] Declan McIntosh and Alexandra Branzan Albu. Inter-realization channels: Unsupervised anomaly detection beyond one-class classification. In *IEEE/CVF International Conference on Computer Vision*, 2023. 3
- [28] Debarghya Mukherjee, Aritra Guha, Justin M Solomon, Yuekai Sun, and Mikhail Yurochkin. Outlier-robust optimal transport. In *International Conference on Machine Learning*, 2021. 3
- [29] Karsten Roth, Latha Pemula, Joaquin Zepeda, Bernhard Schölkopf, Thomas Brox, and Peter Gehler. Towards total recall in industrial anomaly detection. In *IEEE/CVF Conference on Computer Vision and Pattern Recognition*, 2022. 1, 2, 3, 4, 6, 7, 8
- [30] Lukas Ruff, Robert Vandermeulen, Nico Goernitz, Lucas Deecke, Shoaib Ahmed Siddiqui, Alexander Binder, Emmanuel Muller, and Marius Kloft. Deep one-class classification. In *International Conference on Machine Learning*, 2018. 2
- [31] Mohammadreza Salehi, Niousha Sadjadi, Soroosh Baselizadeh, Mohammad H Rohban, and Hamid R Rabiee. Multiresolution knowledge distillation for anomaly detection. In *IEEE/CVF Conference on Computer Vision and Pattern Recognition*, 2021. 6, 7
- [32] Yongyi Su, Xun Xu, and Kui Jia. Revisiting realistic test-time training: Sequential inference and adaptation by anchored clustering. *Advances in Neural Information Processing Systems*, 2022. 2, 4, 6, 7, 8
- [33] Yongyi Su, Xun Xu, Tianrui Li, and Kui Jia. Revisiting realistic test-time training: Sequential inference and adaptation by anchored clustering regularized self-training. 2024. 2, 4, 7
- [34] Hui Tang, Ke Chen, and Kui Jia. Unsupervised domain adaptation via structurally regularized deep clustering. In *IEEE/CVF Conference on Computer Vision and Pattern Recognition*, 2020. 2
- [35] Tran Dinh Tien, Anh Tuan Nguyen, Nguyen Hoang Tran, Ta Duc Huy, Soan Duong, Chanh D Tr Nguyen, and Steven QH Truong. Revisiting reverse distillation for anomaly detection. In *IEEE/CVF Conference on Computer Vision and Pattern Recognition*, 2023. 2
- [36] Chengjie Wang, Wenbing Zhu, Bin-Bin Gao, Zhenye Gan, Jiangning Zhang, Zhihao Gu, Shuguang Qian, Mingang Chen, and Lizhuang Ma. Real-iad: A real-world multi-view dataset for benchmarking versatile industrial anomaly detection. In *IEEE/CVF Conference on Computer Vision and Pattern Recognition*, 2024. 5
- [37] Yue Wang, Jinlong Peng, Jiangning Zhang, Ran Yi, Yabiao Wang, and Chengjie Wang. Multimodal industrial anomaly detection via hybrid fusion. In *IEEE/CVF Conference on Computer Vision and Pattern Recognition*, 2023. 2, 6, 7
- [38] Guoyang Xie, Jinbao Wang, Jiaqi Liu, Feng Zheng, and Yaochu Jin. Pushing the limits of fewshot anomaly detection in industry vision: Graphcore. In *International Conference on Learning Representations*, 2023. 1, 2
- [39] Shiqi Yang, Yaxing Wang, Joost Van De Weijer, Luis Heranz, and Shangling Jui. Generalized source-free domain adaptation. In *IEEE/CVF International Conference on Computer Vision*, 2021. 2
- [40] Xincheng Yao, Chongyang Zhang, Ruoqi Li, Jun Sun, and Zhenyu Liu. One-for-all: Proposal masked cross-class anomaly detection. In *AAAI Conference on Artificial Intelligence*, 2023. 2
- [41] Zhiyuan You, Lei Cui, Yujun Shen, Kai Yang, Xin Lu, Yu Zheng, and Xinyi Le. A unified model for multi-class anomaly detection. In *Advances in Neural Information Processing Systems*, 2022. 6, 7, 8
- [42] Vitjan Zavrtanik, Matej Kristan, and Danijel Skočaj. Draem-a discriminatively trained reconstruction embedding for surface anomaly detection. In *IEEE/CVF International Conference on Computer Vision*, 2021. 2
- [43] Jiangning Zhang, Xuhai Chen, Yabiao Wang, Chengjie Wang, Yong Liu, Xiangtai Li, Ming-Hsuan Yang, and Dacheng Tao. Exploring plain vit reconstruction for multi-class unsupervised anomaly detection. *arXiv preprint*, 2023. 5, 7
- [44] Xinyi Zhang, Naiqi Li, Jiawei Li, Tao Dai, Yong Jiang, and Shu-Tao Xia. Unsupervised surface anomaly detection with diffusion probabilistic model. In *IEEE/CVF International Conference on Computer Vision*, 2023. 1
- [45] Ximiao Zhang, Min Xu, and Xiuzhuang Zhou. Realnet: A feature selection network with realistic synthetic anomaly for anomaly detection. In *IEEE/CVF Conference on Computer Vision and Pattern Recognition*, 2024. 2